Preparation and Study of the Electrochemical Properties of Magnesium Phosphate Membranes

Mohammad Mujahid Ali Khan, Rafiuddin

Membrane Research Laboratory, Department of Chemistry, Aligarh Muslim University, Aligarh 202002, India

Received 5 November 2010; accepted 27 December 2010
DOI 10.1002/app.34103
Published online 5 February 2012 in Wiley Online Library (wileyonlinelibrary.com).

ABSTRACT: Polystyrene-based magnesium phosphate membranes were prepared by a sol–gel method with various 1 : 1 electrolytes at different pressures and concentrations. The prepared membranes were characterized for thickness, porosity, and moisture content and by Fourier transform infrared (FTIR) spectroscopy and scanning electron microscopy (SEM). The FTIR spectra showed a negative shift from the normal polystyrene value due to interaction with metal ions. SEM images revealed nonpreferential orientation without any visible cracks. Teorell, Meyer, and Sievers's method was used to determine the transport number of ions, mobility, distribution coefficient, and charge density of the membrane. The order of surface charge density for a 1 : 1 electrolyte solution was found to be KCl > NaCl > LiCl. However, the membrane potential followed the reverse order. The membrane was found to be stable in acidic and basic environments. This study demonstrated the potential applications of inorganic precipitate membranes in the field of separation science. © 2012 Wiley Periodicals, Inc. J Appl Polym Sci 124: E338–E346, 2012

Key words: charge transport; density; FT-IR; membranes; morphology

INTRODUCTION

Composite materials based on organic polymer matrix–inorganic precipitate ion exchangers are attractive materials in membrane science and technology, as they possess mechanical stability because of the presence of organic polymeric species and the basic characteristics of an inorganic ion exchanger with regard to its selectivity for some particular metal ions.[1–7] The synthesis of a hybrid ion exchanger (via sol–gel methods) with controlled functionality and hydrophobicity could open new opportunities for organometallic chemistry, catalysis, organic host–guest chemistry,[8] analytical chemistry, hydrometallurgy, antibiotic purification, and separation of radioactive isotopes and could find large-scale applications in water treatment and pollution control.[9]

Membrane systems also played a vital role in the purification of the earliest biotechnology products,[10,11] and these were developed for blood fractionation and the food, dairy and distillery industries.[12] Important applications of these membranes include the solution of two environmental problems, the recovery and enrichment of valuable ions and the removal of undesirable ions from wastewater.[9]

Membrane potential studies have commonly been used in the electrochemical characterization of membranes.[13,14] There are various parameters governing the membrane phenomenon. Among these parameters, the surface charge density ($\overline{D}$) is the most effective; it controls the membrane phenomena and can be calculated with the membrane potential values for different electrolytes with the Teorell–Meyer–Sievers (TMS) method.[15–18] Some other parameters, including the distribution coefficient, transport numbers, mobility ratio, and charge effectiveness, were also calculated for polystyrene-based magnesium phosphate membranes.

Polystyrene-based magnesium phosphate membranes exhibit a large number of applications, which make them attractive for filtration tasks in the beverage and textile industry, medicine, pharmacy, chemical industry, wastewater treatment, and others. These applications are attributed to their high thermal resistance, chemical resistance, and mechanical strength.[19]

In this study, we prepared and characterized magnesium phosphate membranes via a sol–gel approach using polystyrene as a binder by the application of different pressures. The values for the membrane potential were inversely proportional to electrolyte concentration, that is, they increased with a decrease in the external electrolyte concentration. This showed that the membranes were cation selective.

THEORY

Fixed charge density theory of TMS

In the TMS theory, there is an equilibrium process at each solution–membrane interface, which has a

Correspondence to: Rafiuddin (rafi_amu@rediffmail.com).
Contract grant sponsor: University Grant Comission (UGC).

formal analogy with the Donnan equilibrium. The assumptions made are that (1) the cation and anion mobilities and fixed charge concentration are constant throughout the membrane phase and are independent of the salt concentration and (2) the transference of water may be neglected. The implications of these assumptions have been discussed.[14] A further assumption, that the activity coefficient of the salt is the same in the membrane and solution phase at each interface, must also be made. The introduction of activities for concentrations can only be corrected by the Donnan potential ($\Delta\overline{\Psi}_{\mathrm{Don}}$) with the integration of either the Planck or Henderson equation. According to TMS theory, the membrane potential ($\Delta\overline{\Psi}_{m,e}$) applicable to a highly idealized system is given by the following equation at 25°C:

$$\Delta\bar{\Psi}_{m,e} = 59.2\left(\log\frac{C_2}{C_1}\frac{\sqrt{4C_1^2+\bar{D}^2}+\bar{D}}{\sqrt{4C_2^2+\bar{D}^2}+\bar{D}} + \bar{U}\log\frac{\sqrt{4C_2^2+\bar{D}^2}+\bar{D}\bar{U}}{\sqrt{4C_1^2+\bar{D}^2}+\bar{D}\bar{U}}\right) \quad (1)$$

$$\bar{U} = (\bar{u}-\bar{v})/(\bar{u}+\bar{v})$$

where $\bar{U}$ is the ratio of difference and sum of ionic mobilities of cation and anion in the membrane; $\bar{u}$ and $\bar{v}$ are the ionic mobilities of the cation and anion ($m^2/v/s$), respectively, in the membrane phase; C_1 and C_2 are the concentrations of the membrane; and $\overline{D}$ is the charge density of the membrane (equiv/L). The graphical method of TMS determines the fixed $\overline{D}$ (equiv/L) and the cation-to-anion mobility ratio in the membrane phase ($\overline{\omega}$).

EXPERIMENTAL

Preparation of the membranes

Magnesium phosphate precipitate was prepared by the mixture of 0.2*M* magnesium (II) chloride (99.98% purity, E. Merck, Mumbai, India) with 0.2*M* trisodium phosphate (99.90% purity, E. Merck, Mumbai, India) in a 100-mL solution. The precipitate was washed well with deionized water (water purification system, Integrate, Lucknow, Uttar Pradesh, India, whose RO conductivity was 0–200 μs/cm and Uttar Pradesh (UP) resistivity was 1–18.3 M Ω cm) to remove free electrolyte and then dried and powdered. Membranes with a suitable ratio of binder (1 : 3) were prepared.[20] The precipitate was ground into a fine powder and sieved through 200-mesh Bronze Standard Sieve (BSS) standard (granule size < 0.07 mm). Pure crystalline polystyrene (Otto Kemi, India, analytical-reagent grade) was also ground and sieved through 200 mesh. The magnesium phosphate, along with an appropriate amount of polystyrene powder, was mixed thoroughly with a mortar and pestle. The mixture was then kept in a cast die having a diameter of 2.45 cm and placed in an oven (Oven–Universal, Memmert type) maintained at 200°C for about 1 h to equilibrate the reaction mixture.[21,22] The die containing the mixture was then transferred to a pressure device (SL-89, London, United Kingdom), and various pressures, including 100, 120, 140, and 160 MPa, were applied during the fabrication of the membranes.

Our effort was to prepare membranes of adequate chemical and mechanical stabilities. The membranes that we prepared by embedding 25% polystyrene were found to be mechanically the most stable and gave reproducible results. Those containing larger amounts (>25%) of polystyrene did not give reproducible results, whereas the one containing smaller amounts (<25%) were found unstable.[23] The total amount of the mixture used for the preparation of the membrane contained 0.125 g of polystyrene (200 mesh) and 0.375 g of magnesium phosphate (200 mesh). The membranes were subjected to microscopic and electrochemical examinations for cracks and homogeneity of the surface, and only those which had a smooth surface and generated reproducible potentials were considered.

Measurement of the membrane potential

The membrane potential was measured with a digital potentiometer (Electronics India, model 118, Chandigarh, Punjab, India). The freshly prepared charged membrane was installed at the center of the measuring cell, which had two glass containers, on either side of the membrane. The various salt solutions (chlorides of K^+, Na^+, and Li^+) were prepared from BDH (analytical-reagent grade) chemicals with deionized water. Both collared glass containers had cavities for introducing the electrolyte solution and saturated calomel electrodes (SCEs). The half-cell contained 25 mL of the electrolyte solution, whereas the capacity of each of the half cells holding the membrane was about 35 mL. The electrochemical setup used for uni-ionic potential and membrane potential measurements may be depicted as follows:

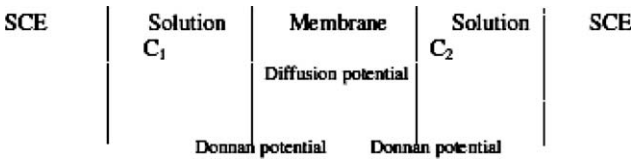

Characterization of the membrane

The prerequisite criterion for understanding the performance of an ion-exchange membrane is its complete physicochemical characterization, which involves the determination of all such parameters

TABLE I
Observed Membrane Potential (mV) across the Magnesium Phosphate Membranes in Contact with Various 1 : 1 Electrolytes at Different Concentrations and Pressures at 25 ± 1°C

	Applied pressure											
	100 (MPa)			120 (MPa)			140 (MPa)			160 (MPa)		
	Membrane potential (mV)											
C_2 (mol/L)	KCl	NaCl	LiCl	KCl	NaCl	LiCl	KCl	NaCl	LiCl	KCl	NaCl	LiCl
−1	7.5	8.6	9.5	8.5	9.5	10.7	9.4	10.2	11.6	10.5	11.2	12.5
—0.1	11.2	12.3	13.1	12.0	13.2	14.2	12.8	13.5	14.5	13.4	14.5	15.6
—0.01	24.4	26.8	27.2	25.5	27.6	28.4	26.2	28.3	28.6	26.8	29.5	30.4
—0.001	48.2	49.4	50.6	49.0	50.2	51.5	49.6	50.8	52.5	50.4	51.6	53.2
—0.0001	52.0	53.2	54.4	52.6	53.9	55.0	53.3	54.6	55.7	54.6	55.8	56.4

that affect its electrochemical properties. These parameters were the membrane water content, porosity, thickness, swelling, and so on. These were determined as described elsewhere.[8]

Water content (total wet weight percentage)

The conditional membrane was first soaked in water, blotted quickly with Whatman filter paper to remove surface moisture, and immediately weighed. These were further dried to a constant weight in a vacuum over P_2O_5 (dehydrating agent) for 24 h. The water content (total wet weight) was calculated as follows:

$$\text{Total (wet wt \%)} = \frac{W_w - W_d}{W_w} \times 100$$

where W_w is the weight of the soaked/wet membrane and W_d is the weight of the dry membrane.

Porosity

Porosity was determined as the volume of water incorporation in the cavities per unit membrane volume from the water content data:

$$\text{Porosity} = \frac{W_w - W_d}{AL\rho_w}$$

where A is the area of the membrane, L is the thickness of the membrane, and ρ_w is the density of water.[24]

Thickness

We measured the thickness of the membrane by taking the average thickness of the membrane with screw gauze.

Swelling

Swelling was measured in accordance with the procedure described by Arfin and Rafiuddin.[24] It was calculated as the difference between the average thicknesses of the membrane equilibrated with 1*M* NaCl for 24 h and that of the dry membrane.

Chemical stability

Chemical stability was evaluated on the basis of the ASTM D 543-m95 method. The membrane was exposed to several media that are commonly used. The membrane was evaluated after 24, 48, and 168 h; we analyzed alterations in color, texture, brightness, decomposition, splits, holes, bubbles, curving, and stickiness.[25]

Scanning electron microscopy (SEM) investigation of the membrane morphology

SEM imaging was used to confirm the microstructure of the fabricated porous membrane. The membrane morphology was investigated by a ZEISS EVO series scanning electron microscope EVO 50, Portland, Oregon, USA at an accelerating voltage of 20 kV. The sample was mounted on a copper stub and sputter-coated with gold to minimize the charging.

Fourier transform infrared (FTIR) spectra of the membrane

The IR spectrum of the magnesium phosphate membrane was done by an Interspec 2020 FTIR spectrometer (Spectrolab, London, United Kingdom). The sample compartment was 200 mm wide, 290 mm deep, and 255 mm high. The entrance and exit beam to the sample compartment was sealed with a coated KBr window, and there was a hinged cover to seal it from the environment.

RESULTS AND DISCUSSION

The values of the observed membrane potentials, measured across magnesium phosphate polystyrene based membranes in contact with various 1 : 1 electrolyte solutions at 25 ± 1°C, are given in Table I. These values were found to be concentration

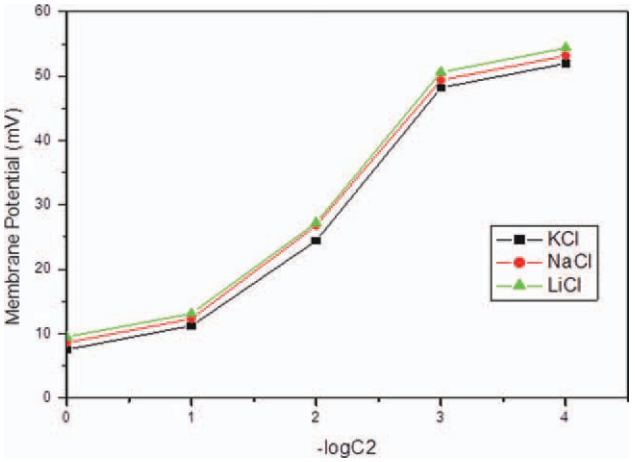

Figure 1 Plots of the observed membrane potentials against the logarithm of concentration for magnesium phosphate membrane with various 1 : 1 electrolytes at 100 MPa of pressure. [Color figure can be viewed in the online issue, which is available at wileyonlinelibrary.com.]

dependent. At low concentration, the potential was found to be high, whereas with increasing concentration of electrolytes, the potential decreased. The membrane potential offered by the various 1 : 1 electrolytes followed the order LiCl > NaCl > KCl. Our results were similar to those reported in the literature.[26] The low observed membrane potential was usual behavior for magnesium phosphate membranes, and therefore, the magnesium phosphate membrane was cation selective.

The membrane potential was also seen to be largely dependent on the applied pressure during membrane formation.[20] The application of high pressure on the magnesium phosphate membranes caused a reduction in thickness, a contraction in pore volume, and consequently, a progressively higher fixed $\overline{D}$,[27,28] which in turn led to a higher membrane potential, as shown in Table I.

Inorganic precipitate membranes were found to have the ability to generate potentials when interposed between electrolyte solutions of different concentrations because of the presence of a net charge on the membranes.[29,30] These charges play crucial role in the transport of electrolytes.[31] The membrane potential data obtained with magnesium phosphate membranes with various 1 : 1 electrolytes were plotted as a function of $-\log C_2$ (Fig. 1).

The results of the thickness, swelling, porosity, and water content capacity measurements of the magnesium phosphate membranes are summarized in Table II. The water content of a membrane depends on the vapor pressure of the surroundings. In case of most of transport measurements, only the membrane water content at saturation is needed and that, too, mostly as a function of solute concentration. Thus, a low order of water content, swelling, and porosity with a lower membrane thickness suggests that the interstices are negligible and diffusion across the membrane would occur mainly through exchange sites.[24]

The membranes were tested for chemical resistance in acidic, alkaline, and strongly oxidant media. In acidic (1*M* H_2SO_4) and alkaline (1*M* NaOH) media, few significant modifications were observed after 24, 48, and 168 h; this demonstrated that the membrane was quite effective in such media. However, in strong oxidant media, the synthesized membrane became fragile in 48 h and broken after 168 h, losing mechanical strength. In general, membranes having the same chemical composition were found to absorb the same amount of water, where density ionizable groups were the same throughout the membrane.[32] Moreover, in membrane transport phenomenon, the membrane water content as a function of solute concentration at saturation is needed. Thus, a low order of water content, swelling, and porosity with a lower membrane thickness suggested that the interstices were negligible and diffusion across the membrane occurred mainly through exchange sites.

The characterization of membrane morphology has been studied by a number of investigators using SEM.[33,34] The surface morphologies of the membranes showed a uniform arrangement of particles, whereas cross-sectional SEM images showed no visible cracks. The composite pore structure, microporosity/macroporosity, homogeneity, thickness, cracks, and surface texture/morphology have been studied.[35,36] The SEM, surface, and cross-sectional images of the magnesium phosphate membranes prepared at 100, 140, and 120 MPa of applied pressure, respectively, are shown in Figures 2(a–c) and 3.

TABLE II
Characterization of the Magnesium Phosphate Membranes

Applied pressure (MPa)	Thickness of the membrane (cm)	Water content (wt % of the wet membrane)	Porosity	Swelling (wt % of the wet membrane)
100	0.090	0.10	0.14	No swelling
120	0.085	0.08	0.12	No swelling
140	0.080	0.06	0.09	No swelling
160	0.075	0.04	0.06	No swelling

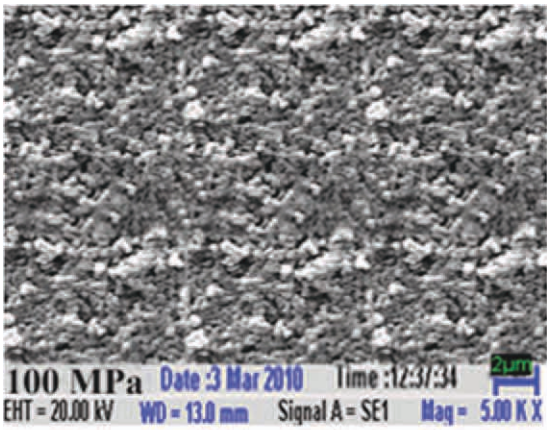

(a)

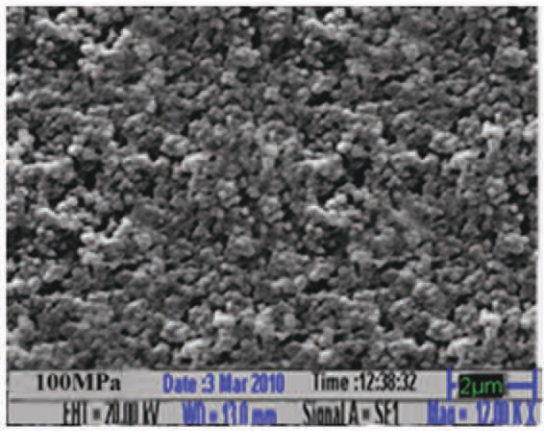

(b)

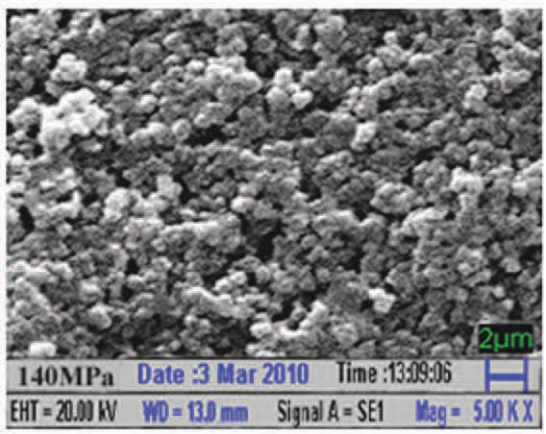

(c)

Figure 2 SEM images of the polystyrene-based magnesium phosphate membranes at (a) 100 MPa and 5000×, (b) 100 MPa and 12,000×, and (c) 140 MPa and 5000×. [Color figure can be viewed in the online issue, which is available at wileyonlinelibrary.com.]

SEM images provided ideas regarding the preparation of well-ordered crack-free membranes. The membranes had random nonpreferential orientation with no visible cracks and appeared to be composed of dense and loose aggregations of small particles. The SEM image was dense in nature and formed pores probably with a nonlinear channel but not fully interconnected. The particles were irregularly condensed and adopted a heterogeneous structure composed of masses of various sizes. Because of the strong interactions between the styrene particles and the membrane pore walls, the particles did not permeate through the membrane.

The distributions of $\overline{D}$ and mobile species within the pores were assumed to be uniform. The diameters of the polystyrene particles were clearly much smaller than the pore diameters of the membrane used.[37]

Inorganic composite membranes have the ability to generate potential when two electrolyte solutions of unequal concentration are separated by a membrane and driven by different chemical potential acting across the membrane.[38,39] The migration of charged species is regulated by the electrical behavior of the membrane, and the diffusion of electrolytes from higher to lower concentration takes place through the charged membrane. In fact, the mobile species penetrate into the membrane at different magnitudes, and various transport phenomena, including the development of potentials across it, are induced into the system.[40] The fixed-charge concept of the TMS model[15–18] for a charged membrane is an appropriate starting point for the investigations of the actual mechanisms of ionic or molecular processes that occur in the membrane phase. The membrane potential applicable to an idealized system according to TMS is represented by eq. (1).

The $\overline{D}$ values of inorganic membranes were estimated from the membrane potential measurement

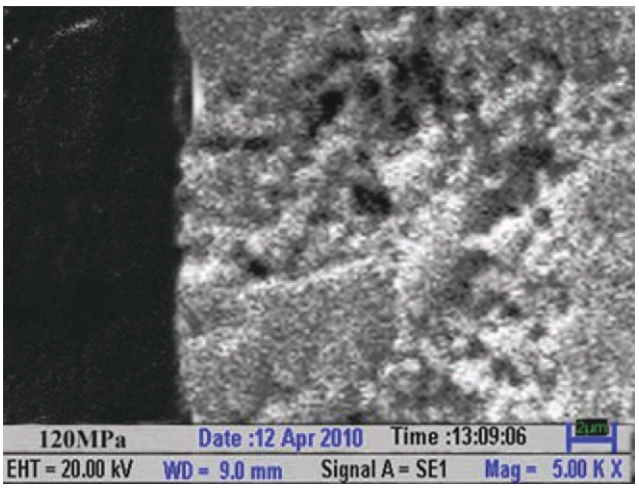

Figure 3 SEM image of the polystyrene-based magnesium phosphate membrane at 120 MPa and 12,000× (cross-sectional view). [Color figure can be viewed in the online issue, which is available at wileyonlinelibrary.com.]

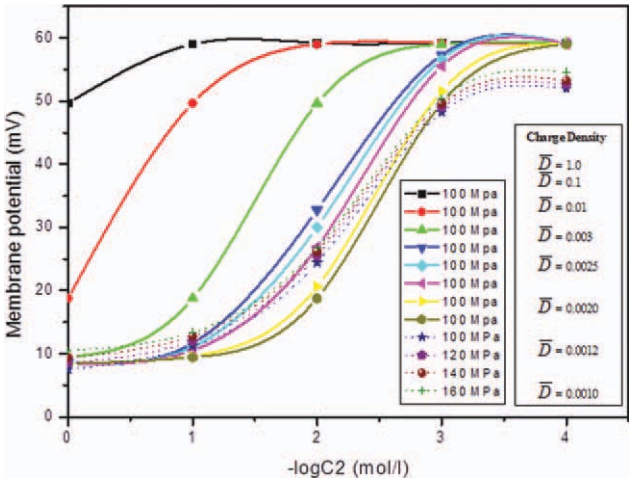

Figure 4 Plots of the membrane potential (mV) versus $-\log C_2$ (mol/L) at different concentrations of KCl electrolyte solution for magnesium phosphate membranes prepared at different pressures of 100–160 MPa. [Color figure can be viewed in the online issue, which is available at wileyonlinelibrary.com.]

and could also be estimated from the transport number. To evaluate this parameter for the simple case of a 1 : 1 electrolyte and a membrane carrying various $\overline{D}$'s of 1 or less, the theoretical potential and observed potential were plotted as a function of $-\log C_2$, as shown by solid and broken lines, respectively, in Figure 4. Thus, the coinciding curve for various electrolyte systems gave the value of $\overline{D}$ within the membrane phase, as shown in Table III. $\overline{D}$ of magnesium phosphate membranes was found to depend on the applied pressure to which the membrane was subjected to its initial stage of preparation.

The thickness of the magnesium phosphate membranes diminished continuously from 0.090 to 0.075 cm with a progressive increase in the applied pressure. The increase in the values of $\overline{D}$ with higher applied pressure was due to the successive increase of charges per unit volume and the decrease in pore volume of the magnesium phosphate membranes, and therefore, the degree of selectivity for ions was enhanced with the modification in the surface microstructure of the membrane.

TABLE III
Derived Values of $\overline{D}$ ($\times 10^{-3}$ equiv/L) for Various Magnesium Phosphate Membrane Electrolyte Systems as Calculated with the TMS Equation

Applied pressure (MPa)	$\overline{D} \times 10^{-3}$		
	KCl	NaCl	LiCl
100	1.41	1.19	0.09
120	1.74	1.31	1.10
140	1.83	1.42	1.25
160	2.07	1.73	1.31

$\overline{D}$ values of the membranes with 1 : 1 electrolytes (KCl, NaCl and LiCl) were plotted against the pressures (Fig. 5), and the order of $\overline{D}$ values for the electrolytes used was found to be KCl > NaCl > LiCl.

The TMS eq. (1) can also be expressed by the sum of $\Delta\overline{\Psi}_{\text{Don}}$ values between the membrane surfaces and the external solutions and the diffusion potential ($\Delta\overline{\Psi}_{\text{diff}}$) within the membrane:[41,42]

$$\Delta\bar{\Psi}_{m,e} = \Delta\Psi_{\text{Don}} + \Delta\bar{\Psi}_{\text{diff}} \tag{2}$$

$$\Delta\psi_{\text{Don}} = -\frac{RT}{V_k F}\ln\left(\frac{\gamma_{2\pm}C_2\bar{C}_{1+}}{\gamma_{1\pm}C_1\bar{C}_{2+}}\right) \tag{3}$$

where R is the gas constant (J/K/mol), T is the temperature, F is the Faraday constant (C/mol), $\gamma_{1\pm}$ and $\gamma_{2\pm}$ are the mean ionic activity coefficients, and $\overline{C}_{1+}$ and $\overline{C}_{2+}$ are the cation concentrations in the first and second membrane phases, respectively. The cation concentration is given by the following equation:

$$\bar{C}_+ = \sqrt{\left(\frac{V_x\bar{D}}{2V_k}\right)^2 + \left(\frac{\gamma_\pm C}{q}\right)^2} - \frac{V_x\bar{D}}{2V_k} \tag{4}$$

where V_k and V_x refer to the valencies of the cation and fixed-charge group on the membrane matrix, $\gamma_\pm$ is the mean ionic activity coefficient, and q is the charge effectiveness of the membrane and is defined by the following equation:

$$q = \sqrt{\frac{\gamma_\pm}{K_\pm}} \tag{5}$$

where $K_\pm$ is the distribution coefficient, expressed as

$$K_\pm = \frac{\bar{C}_i}{C_i},\ \bar{C}_i = C_i - \bar{D} \tag{6}$$

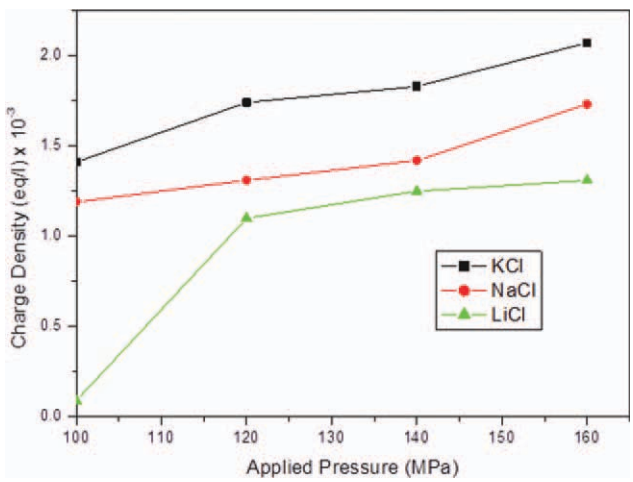

Figure 5 Plot of $\overline{D}$ of the magnesium phosphate membrane for the 1 : 1 electrolytes (KCl, NaCl, and LiCl) versus the pressure. [Color figure can be viewed in the online issue, which is available at wileyonlinelibrary.com.]

TABLE IV
Values of t_+, $\overline{U}$, $\overline{\omega}$ and $K_\pm$, q, and $\overline{C}_+$ Evaluated with eqs. (9), (6), (5), and (4), Respectively, from the Observed Membrane Potentials for Various Electrolytes at Different Concentrations for Magnesium Phosphate Membranes Prepared at 100 MPa of Pressure

C_2 (mol/L)	t_+	$\overline{U}$	$\overline{\omega}$	$K_\pm$	q	$\overline{C}_+$
KCl (electrolyte)						
1.000	0.57	0.14	1.32	0.998	1.002	0.9965
0.1000	0.59	0.18	1.43	0.985	1.015	0.0971
0.0100	0.71	0.42	2.44	0.859	1.164	0.0072
0.0010	0.91	0.82	10.1	−0.410	2.439	5.8401
0.0001	0.94	0.88	15.6	−13.100	0.076	0.0005
NaCl						
1.000	0.58	0.61	1.38	0.999	1.001	0.9988
0.1000	0.61	0.22	1.56	0.998	1.002	0.0996
0.0100	0.73	0.46	2.70	0.981	1.019	0.0096
0.0010	0.92	0.84	11.5	0.810	1.234	0.0006
0.0001	0.96	0.92	24.0	0.900	1.111	0.00002
LiCl						
1.000	0.59	0.18	1.43	0.999	1.001	0.9980
0.1000	0.62	0.24	1.63	0.990	1.010	0.0980
0.0100	0.74	0.48	2.84	0.902	1.108	0.0080
0.0010	0.93	0.86	13.2	0.020	50.000	0.00000002
0.0001	0.97	0.94	32.3	−8.800	0.113	0.0003

where $\overline{C}_i$ is the ith ion concentration in the membrane phase and C_i is the ith ion concentration of the external solution. The transport of electrolyte solutions in pressure-driven membrane showed that the transport properties of the membrane were also controlled by ion distribution coefficients. It appeared that the use of eq. (6) for evaluating the distribution coefficients gave low values at lower concentrations, and as the concentration of electrolytes increased, the value of distribution coefficients sharply increases and thereafter, a stable trend was observed, which is presented in Table IV.

$\Delta\overline{\Psi}_{\text{diff}}$ is expressed in the following form:

$$\Delta\bar{\Psi}_{\text{diff}} = -\frac{RT}{V_k F}\frac{\bar{\omega}-1}{\bar{\omega}+1} \times \ln\left(\frac{(\bar{\omega}+1)\bar{C}_{2+} + (V_x/V_k)\bar{D}}{(\bar{\omega}+1)\bar{C}_{1+} + (V_x/V_k)\bar{D}}\right) \tag{7}$$

where $\overline{\omega} = \overline{u}/\overline{v}$. The total $\Delta\overline{\Psi}_{m,e}$ was thus obtained by the simple addition of eqs. (3) and (7):

$$\Delta\bar{\Psi}_{m,e} - \frac{RT}{V_k F}\ln\left(\frac{\gamma_{2\pm}C_2\bar{C}_{1+}}{\gamma_{1\pm}C_1\bar{C}_{2+}}\right) - \frac{RT}{V_k F}\frac{\bar{\omega}-1}{\bar{\omega}+1} \times \ln\left(\frac{(\bar{\omega}+1)\bar{C}_{2+} + (V_x/V_k)\bar{D}}{(\bar{\omega}+1)\bar{C}_{1+} + (V_x/V_k)\bar{D}}\right) \tag{8}$$

To test the applicability of these theoretical equations for the system under investigation, $\Delta\overline{\Psi}_{\text{Don}}$ and $\Delta\overline{\Psi}_{\text{diff}}$ were calculated separately from the membrane parameters obtained from membrane potential measurements with a typical membrane prepared at a pressure of 100 MPa.

The transport properties of the membrane in various electrolyte solutions are important parameters to further investigate the membrane phenomena, as shown in eq. (9):

$$\Delta\bar{\psi}_m = \frac{RT}{F}(t_+ - t_-)\ln\frac{C_2}{C_1}\frac{t_+}{t_-} = \frac{\bar{u}}{\bar{v}} \tag{9}$$

Equation (9) was first used to get the values of the transport numbers of the cation (t_+) and anion (t_-) from the experimental membrane potential data, and consequently, $\overline{\omega} = \overline{u}/\overline{v}$ and $\overline{U}$ were calculated and are given in Table IV. The mobility ($\overline{\omega}$) of the electrolyte in the membrane phase was found to be high, and the order was LiCl > NaCl > KCl, as shown in Figure 6.

The high mobility was attributed to the higher transport number of comparatively free cations of electrolyte; this was also found to have a similar trend to the mobility in the least concentrated solution. The transport numbers of the cations of the various electrolytes (KCl, NaCl, and LiCl) increased with decreasing concentration of electrolytes and followed the increasing order KCl < NaCl < LiCl, as shown in Figure 7.

$\Delta\overline{\Psi}_{\text{Don}}$ and $\Delta\overline{\Psi}_{\text{diff}}$ at various electrolyte concentrations could be calculated from the parameters $\gamma_{1\pm}$, $\gamma_{2\pm}$, $\overline{C}_{1+}$, $\overline{C}_{2+}$, $\overline{\omega}$, V_x, and V_k, and the experimentally derived values of $\overline{D}$ with eqs. (3) and (7). The values of the parameters $K_\pm$, q, and $\overline{C}_+$ derived for the system are also shown in Table IV. The values of $\gamma_\pm$ were the usual charted values for the electrolytes (KCl, NaCl, and LiCl).

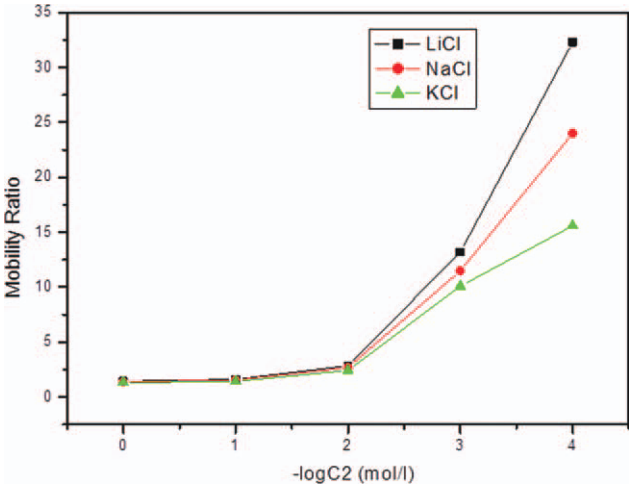

Figure 6 Plot of the mobility ratio of magnesium phosphate membrane for the 1 : 1 electrolytes (KCl, NaCl, and LiCl) versus the concentration. [Color figure can be viewed in the online issue, which is available at wileyonlinelibrary.com.]

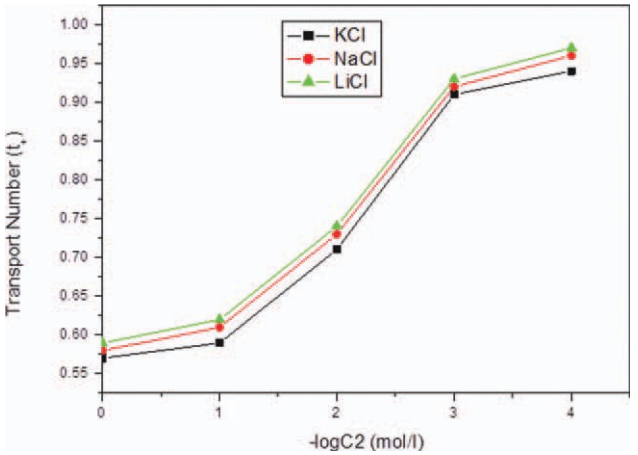

Figure 7 Plot of the transport number of the cation of the magnesium phosphate membrane for the 1 : 1 electrolytes (KCl, NaCl, and LiCl) versus the concentration. [Color figure can be viewed in the online issue, which is available at wileyonlinelibrary.com.]

The FTIR spectra were obtained to ascertain the composition and possible addition sites of the magnesium phosphate membranes. The spectra contained weak to strong intensity peaks assigned to various functional groups in the material synthesized. The peaks showed slight negative shifts in comparison to the free polystyrene or magnesium phosphate membranes. The peaks in the range 696–874 cm^{-1} showed the presence of an aromatic ring in the polystyrene-based magnesium phosphate membrane.[43] The peaks at 2852 and 2927 cm^{-1} supported the C—H bond frequency due to a stirring moiety in the material. The characterization peaks of the phosphate groups present in the region of 1079 cm^{-1} in the IR spectra ascertained the presence of phosphate groups attached to the metal in the composite.[44]

The IR spectra of the polystyrene-based magnesium phosphate membranes, as shown in Figure 8, showed a negative shift for most of the functional groups relative to the noncoordinated free functions.[44] The IR

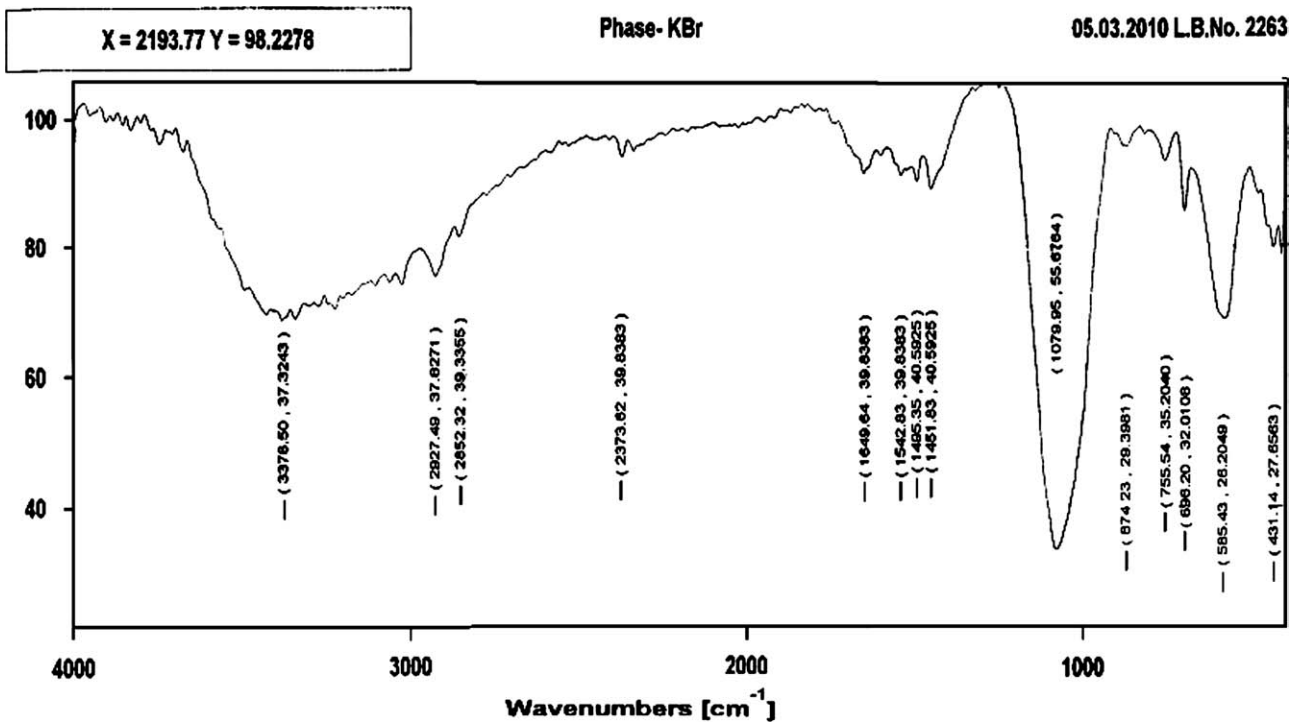

Figure 8 IR spectra of the polystyrene-based magnesium phosphate membrane.

spectral results were in line with the other studies discussed previously, in which the polymeric nature of the composite was confirmed.

CONCLUSIONS

Polystyrene-based magnesium phosphate membranes were prepared by a sol–gel method, and these were found to be quite stable and did not show any dispersion in water or in other electrolyte solutions. The surface charge model could be used as a tool to improve the performance of the membrane filtration process and the selectivity of ion exchange. The membrane potential offered by the electrolytes followed the decreasing order LiCl > NaCl > KCl, and the membranes were found to be cation selective.

The experimental results were analyzed on the basis of the TMS approach. The values of $\overline{D}$ evaluated were the central parameter governing the transport phenomena in the membranes, and it depended on the feed composition and the applied pressure due to the preferential adsorption of some ions; it, in turn, accounted for the performance of the membrane. The order of $\overline{D}$ for the electrolytes used was KCl > NaCl > LiCl.

The authors gratefully acknowledge the Chairman, Department of Chemistry, Aligarh Muslim University, Aligarh (India), for providing necessary research facilities. The authors also thank the Indian Institute of Technology, Delhi, for providing the SEM facility.

References

1. Khan, A. A.; Alam, M. M. React Funct Polym 2003, 55, 277.
2. Varshney, K. G.; Tayal, N.; Khan, A. A.; Niwas, R. Colloid Surf A 2001, 181, 123.
3. Gupta, A. P.; Agarwal, H.; Ikram, S. J Indian Chem Soc 2003, 80, 57.
4. Niwas, R.; Khan, A. A.; Varshney, K. G. Colloid Surf A 1999, 150, 7.
5. Varshney, K. G.; Tayal, N.; Gupta, U. Colloid Surf A 1998, 145, 71.
6. Zhang, B.; Poojary, D. M.; Clearfield, A.; Peng, G. Chem Mater 1996, 8, 1333.
7. Alberti, G.; Casciola, M.; Dionigi, C.; Vivani, R. In Proceedings of International Conference on Ion-Exchange ICIE'95, Takamtsu, Japan, 1995.
8. Khan, A.; Khan, A. A.; Inamuddin. Talanta 2007, 72, 699.
9. Nabi, S. A.; Naushad, M.; Inamuddin. J Hazard Mater 2007, 142, 404
10. Ladisch, M. R.; Kohlmann, K. L. Biotech Prog 1992, 8, 469.
11. Blanch, H. W.; Clark, D. S. Biochemical Engineering; Marcel Dekker: New York, 1997.
12. Kosikowski, F. V. In Membrane Separations in Biotechnology; McGregor, W. C., Ed.; Marcel Dekker, New York, 1975.
13. Singh, K.; Tiwari, A. K. J Membr Sci 1987, 34, 155.
14. Singh, K.; Shahi, V. K. J Membr Sci 1990, 49, 223.
15. Teorell, T. Proc Soc Exp Biol 1935, 33, 282.
16. Teorell, T. Proc Natl Acad Cad Sci (USA) 1935, 21, 152.
17. Meyer, K. H.; Sievers, J. F. Helv Chim Acta 1936, 19, 649; Helv Chim Acta 1936, 19, 665; Helv Chim Acta 1936, 19, 987.
18. Chou, T. J.; Tanioka, A. J Phys Chem B 1998, 102, 7198.
19. Arfin, T.; Rafiuddin, Metal ion transport through a polystyrene-based cobalt arsenate membrane: Application of irreversible thermodynamics and theory of absolute reaction rates, Desalination 2012, 284, 100.
20. Jabeen, F.; Rafiuddin. J Appl Polym Sci 2008, 110, 3023.
21. Beg, M. N.; Siddiqi, F. A.; Singh, S. P.; Prakash, P.; Gupta, V. Electrochem Acta 1979, 24, 85.
22. Beg, M. N.; Siddiqi, F. A.; Shyam, R.; Altaf, I. J Electronal Chem 1978, 89, 141.
23. Arfin, T.; Rafiuddin. Electrochim Acta 2009, 54, 6928.
24. Arfin, T.; Rafiuddin. J Electroanal Chem 2009, 636, 113.
25. Annual Book of Standards; ASTM D 543–95; American Society for Testing and Materials: West Conshohocken, PA, 1998; p 27.
26. Jabeen, F.; Rafiuddin. J Porous Mater 2009, 16, 257.
27. Helfferich, F. Ion-Exchange; McGraw-Hill: New York, 1962.
28. Winter, R.; Czeslik, C. Z Kristalloger 2000, 215, 454
29. Shahi, V. K.; Trivedi, G. S.; Thampy, S. K.; Ranrarajan, R. J Colloid Interface Sci 2003, 262, 566.
30. Chai, J. H.; Moon, S. H. J Membr Sci 2001, 191, 225.
31. Schaep, J.; Vandecasteele, C. J Membr Sci 2001, 188, 129.
32. Koter, S.; Piotrowski, P.; Kerrs, J. J Membr Sci 1999, 153, 83.
33. Liu, J.; Xu, T.; Gong, M.; Yu, F.; Fu, Y. J Membr Sci 2006, 283, 190.
34. Silva, V.; Ruffmann, S. B.; Vetter, S.; Mendes, A.; Madeira, L. M.; Nunes, S. P. Catal Today 2005, 104, 205.
35. Titiloye, J. O.; Hussain, I. J Colloid Interface Sci 2008, 318, 50.
36. Resinaa, M.; Macanása, J.; de Gyvesb, J.; Muñoza, M. J Membr Sci 2007, 289, 150.
37. Aleman, J. G.; Dicker, J. M. J Membr Sci 2004, 235, 1.
38. Eisenman, G. In Membrane Transport and Metabolism; Kleinser, A., Koty, A., Eds.; Academic: New York, 1961; p 163
39. Barragan, V. M.; Rueda, C.; Ruiz-Baura, C. J Colloid Interface Sci 1995, 172, 361.
40. Lakshminarayanaiah, N. Transport Phenomena in Membranes; Academic: New York, 1969.
41. Matsumoto, H.; Tanioka, A.; Murata, T.; Higa, M.; Horiuchi, K. J Phys Chem B 1998, 102, 5011.
42. Chou, T.-J.; Tanioka, A. J Colloid Interface Sci 1999, 212, 293
43. Nakamoto, K. Infrared and Raman Spectra of Inorganic and Coordinate Compounds; Wiley-Interscience: New York, 1986.
44. Bellamy, L. J. The Infra-Red Spectra of Complex Molecules; Chapman & Hall: London, 1975; Vol. 1.